Technical Sciences
Academy of Romania
www.jesi.astr.ro

Journal of Engineering Sciences and Innovation
Volume 7, Issue 1 / 2022, pp. 1 - 14

A. Mechanical Engineering

Received ***26 November 2021*** *Accepted* ***7 March 2022***
Received in revised form ***18 February 2022***

Modal testing of a turbofan case using the LMIF

MIRCEA RADEŞ*

Politehnica University of Bucharest, Splaiul Independenţei 313, Bucharest, Romania

Abstract: In this paper, part of the data collected during the modal survey of a turbofan case is used to assess the performance of a new mode indicator function able to locate the double radial modes. The new *L*-values Mode Indicator Function (LMIF) is based on the pivoted QLP decomposition of the measured Frequency Response Function matrices at discrete frequencies. For freely supported cyclic structures, the radial modes rotate with the largest amplitude at the input point. This allows testing with only one excitation point.

Keywords: pivoted QLP decomposition, turbofan case, L-values, LMIF, QeFRFs.

1. Introduction

A turbofan case is a cyclic structure possessing double modes with identical natural frequencies. When it is freely hanged up, the Frequency Response Functions (FRFs) measured at certain pairs of excitation and response points are identical. This allows testing using only one excitation point. But measured FRFs cannot reveal the double modes. Their presence is detected using Mode Indicator Functions (MIFs) like the Complex Mode Indicator Function [1] and the Multivariate Mode Indicator Function [2]. MIFs are real-valued frequency-dependent scalars that exhibit local minima or maxima at the modal frequencies of the system. They are calculated using measured complex FRFs. Their plots have as many curves as the number of references.
The *pivoted QLP decomposition* of a real matrix was introduced in 1998 by Stewart [3] as an extension of the *pivoted QR decomposition*, with better rank-revealing properties. It was first applied to composite FRF matrices in which all individual measured FRFs were arranged column-wise in a two-dimensional array [4]. In this paper the pivoted QLP decomposition is performed frequency by frequency for complex-valued rectangular FRF matrices, measured at N_o response

*Correspondence address: mircearades@gmail.com

coordinates, N_i input coordinates $(N_i \leq N_o)$ and N_f frequencies. The absolute values of the diagonal elements of the $[L]$ matrix are called L-values. The LMIF is a plot of the L-values versus frequency. It has peaks at the damped natural frequencies. Double modes are revealed by two peaks at the same frequency. The orthonormal columns of matrices $[Q]$ and $[P]$ are used as spatial filters to produce enhanced FRFs for each mode of vibration.

2. Preliminary tests

The receptance FRFs used in this example were calculated from inertance FRFs measured on a turbofan case of diameter 1.22 m. The location of measurement points is depicted in Fig. 1. The case was hanged up at nodes 40 and 46. Tests were done using impact excitation with a hammer instrumented with a force sensor, the response was measured with an accelerometer and FRFs were obtained through conventional techniques.

Preliminary measurements were carried out using three hitting points, 2, 50 and 60, and six response measurement points, 1, 2, 16, 21, 50 and 60. The resulting 18 FRFs have been used to build up complex 6x3 FRF matrices, measured at 801 frequencies, in the range 40 to 440 Hz, with a resolution of 0.5 Hz.

As an axisymmetric structure, the tested case is expected to possess pairs of orthogonal modes at a resonance frequency. This is not revealed by FRFs so that several Mode Indicator Functions have been plotted to reveal the existence of double modes

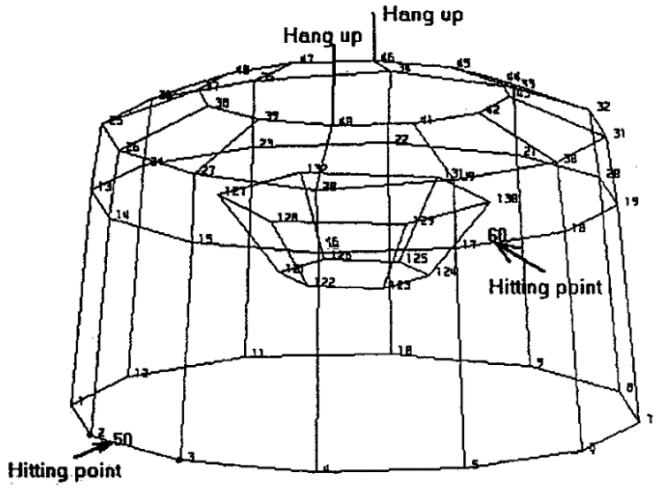

Fig.1. Test structure

The Imaginary Mode Indicator Function (ImMIF) presented in Fig.2 is based on the singular values of the imaginary part of FRF matrices. The ImMIF peaks locate real normal modes.

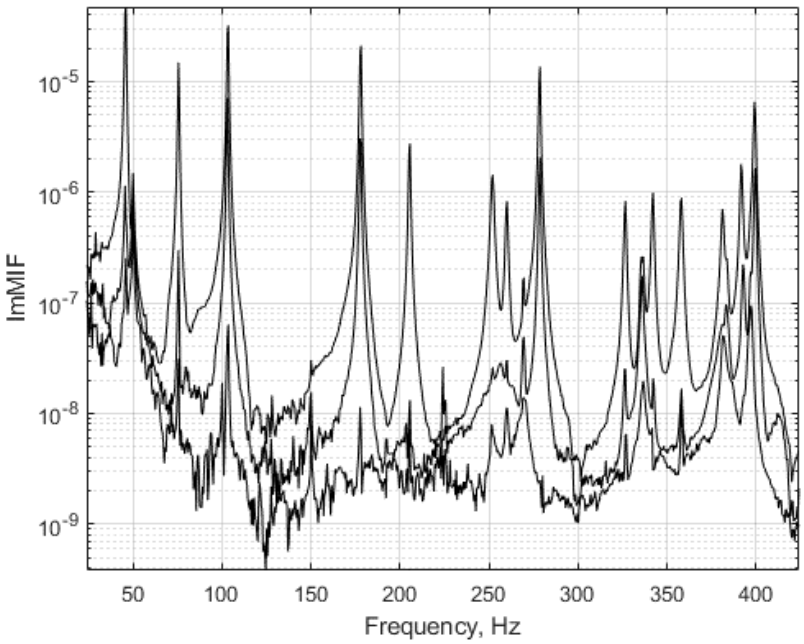

Fig.2. ImMIF plot.

Figure 3 illustrates the Multivariate Mode Indicator Function (MMIF). The MMIF plot exhibits troughs at the undamped natural frequencies.

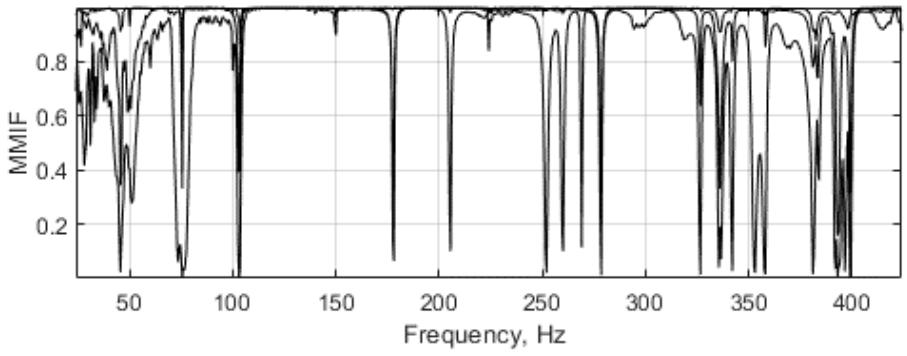

Fig.3. MMIF plot

For comparison, the Complex Mode Indicator Function (CMIF) is depicted in Fig.4. The peaks in the CMIF plot occur at the damped natural frequencies.

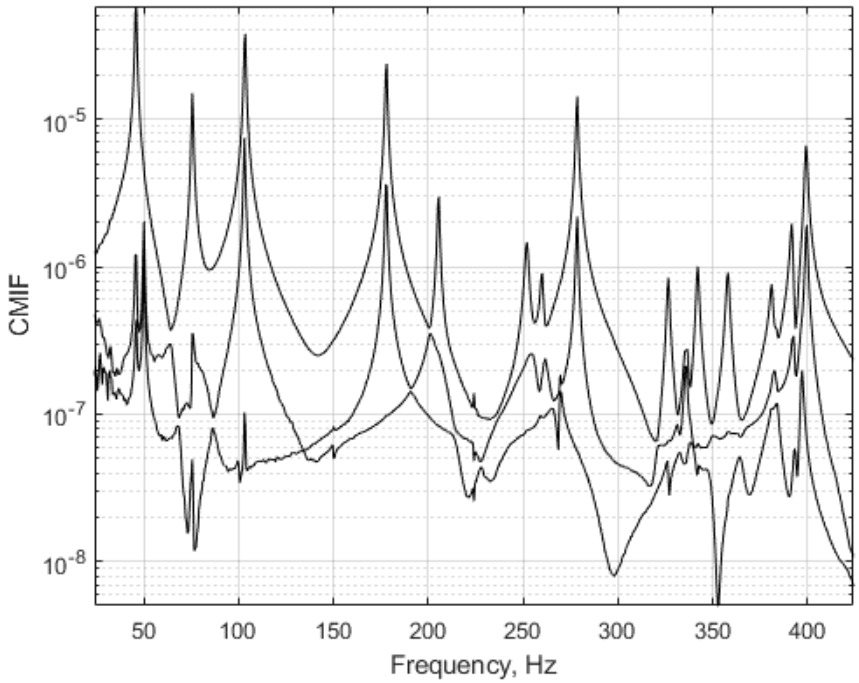

Fig.4. CMIF plot

The analysis of the plots from Figs.2 to 4 have shown that the frequency resolution of 0.5 Hz was too low. To sustain the purpose of this paper, it was decided to restrict measurements to a narrower frequency range, with the same number of discrete frequencies, and to improve the frequency resolution.

2. FRF measurements

Measurements were carried out in the frequency range 24 to 224 Hz, with 0.25 Hz resolution, considering only radial displacements and radial excitation forces. The data selected for the modal analysis were limited to 12 response measurement locations (1 to 12 along the bottom rim) and 3 force input locations (2, 3 and 50). This amounts to 36 complex FRFs, each measured at 801 discrete frequencies.
Receptance frequency response functions $FRFjk = H_{jk}(\omega)$ for displacement at coordinate j produced by excitation at coordinate k are represented as magnitude (log scale) versus frequency (linear scale) plots in Fig.5, for excitation in 2, and in Fig.6, for excitation in 3. The FRF matrices $[H(\omega)]_{N_o \times N_i}$ are measured at N_f frequencies.

Due to reciprocity, the functions $FRF_{23}=FRF_{32}$. Their graphs are identical.

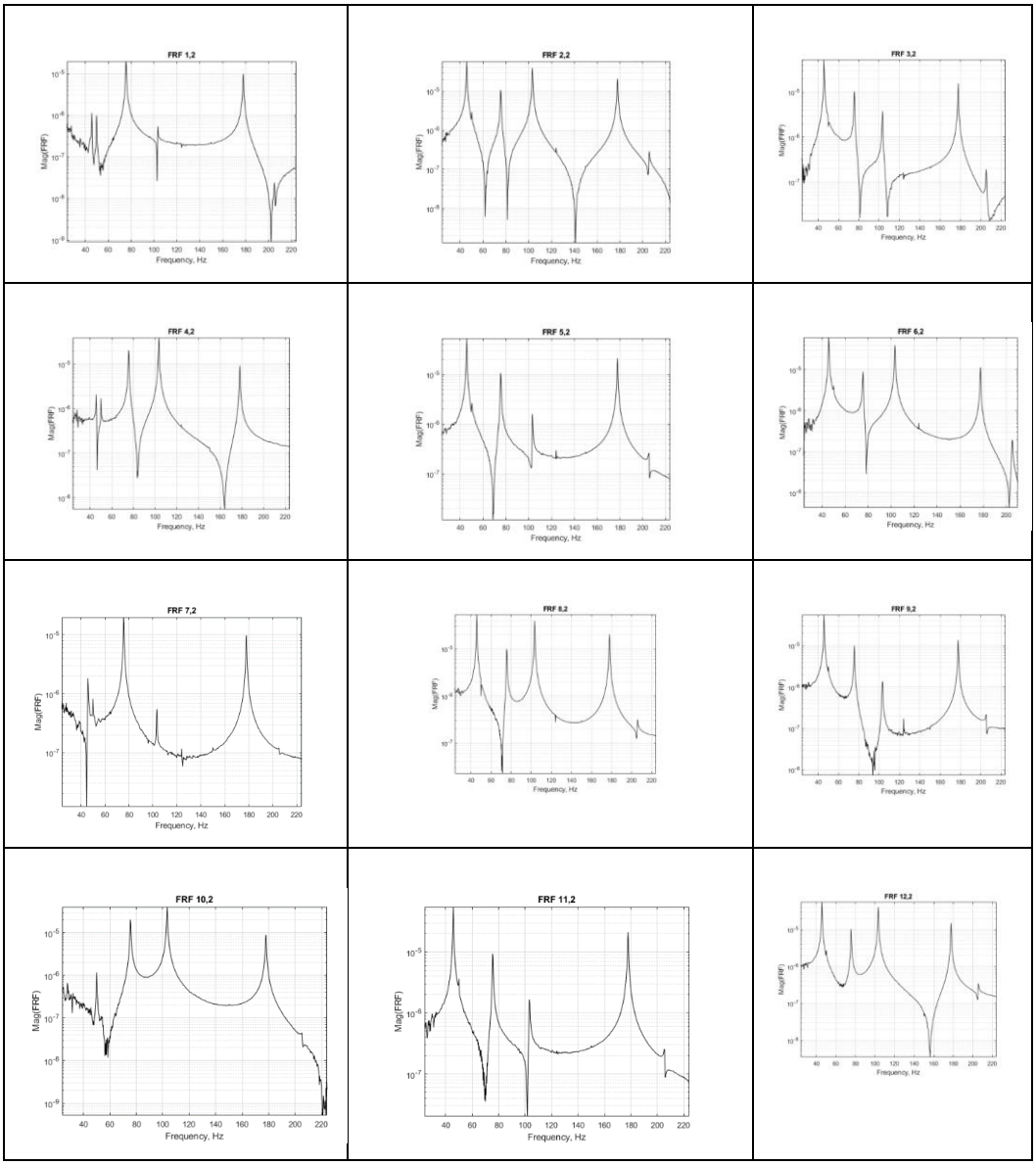

Fig.5. FRFs for excitation in 2

Due to the circular symmetry, the *point* response function *FRF22* is identical to the *point* response function *FRF33*.

The *transfer* FRFs measured for different pairs of excitation and response points with the same circumferential spacing are identical. Examples are the pairs *FRF12*

and *FRF43* (30º apart), *FRF122* and *FRF53* (60º apart), *FRF112* and *FRF63* (90º apart), *FRF102* and *FRF73* (120º apart), *FRF92* and *FRF*83 (150º apart), *FRF82* and *FRF*93 (180º apart), *FRF72* and *FRF103* (210º apart), *FRF62* and *FRF113* (240º apart), *FRF52* and *FRF123* (270º apart), *FRF42* and *FRF13* (300º apart). Small differences are due to inherent measurement errors.

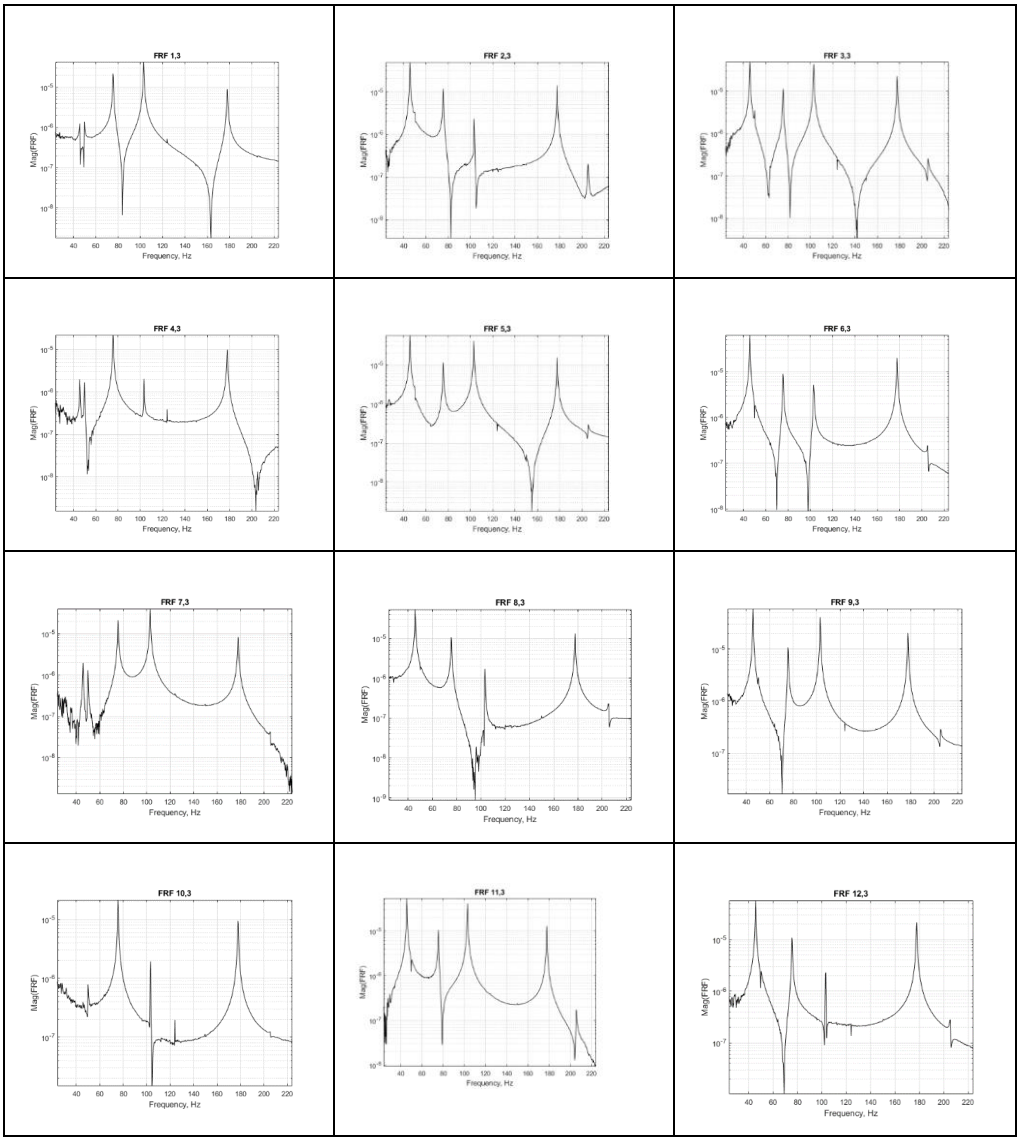

Fig.6. FRFs for excitation in 3

Visual inspection reveals four resonance frequencies, at 45.75, 75.7, 103.3 and 177.8 Hz and a weak mode at 205.5 Hz. It is obvious that such plots cannot reveal double modes.

4. Natural frequencies and mode shapes

The damped natural frequencies, the modal damping ratios and the shapes of the main resonant radial modes, calculated based on FRFs measured using excitation in 3, are given in Fig.7. The mode shapes show the instantaneous value of the imaginary part of the travelling complex modes of a structure with non-proportional damping.

As an axisymmetric structure, the tested casing possesses pairs of orthogonal modes. This is not revealed by simple examination of FRFs. Double modes have identical modal shapes but rotated relatively. A measured mode shape is often a combination of such two modes. Mode indicator functions are used to locate double modes.

$Modal\ frequency, Hz$			
45.75	75.5	103.3	177.8
$Modal\ damping\ ratio, \%$			
0.39	0.26	0.19	0.14
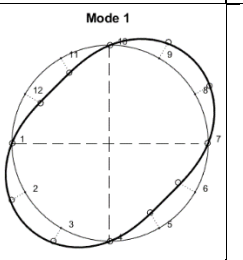	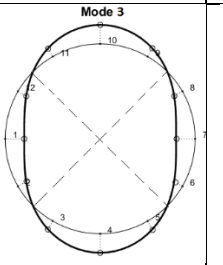	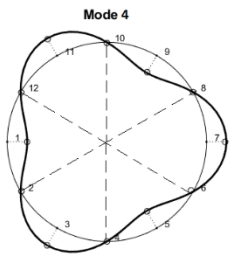	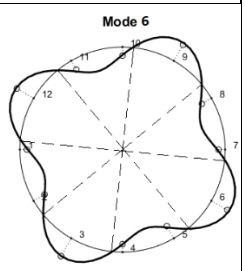

Fig.7. Measured mode shapes for excitation in 3

Mode 1 at 45.75 Hz has two node pairs. It is described by $u = \sin 2\theta$, where θ is the circumferential coordinate measured from point 1. Mode 3 at 75.5 Hz has also two node pairs and a different longitudinal distribution. Mode 4 at 103.3 Hz has three node pairs and the shape $u = \cos 3\theta$. Mode 6 at 177.8 Hz has four node pairs. Mode 8 at 205.3 Hz has two node pairs.

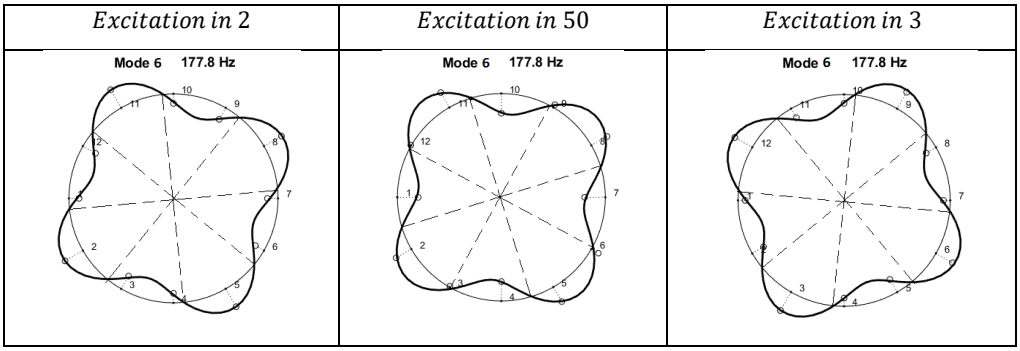

Fig.8. Mode shape at 177.8 Hz, for three different excitation points

For a perfectly symmetric casing there is no preferred orientation of a mode with respect to the free-free structure. It is possible to rotate the mode shape through any angle without changing the frequency of vibration. Usually the modes rotate with the largest element at the driving point. This is illustrated in Fig.8 for the mode at 177.8 Hz calculated for excitation in three different points.

5. Pivoted QLP decomposition of FRF matrices

The Pivoted QLP Decomposition is extended here to complex matrices as an alternative parsimonious description of frequency response data. It is a pivoted orthogonal triangularization, being less expensive and more straightforward than an orthogonal diagonalization like the SVD.

The pivoted QLP decomposition of the FRF matrix $[H]$ can be written

$$[H] = \left[\hat{Q}\right] [L] \left[\hat{P}\right]^H, \qquad (1)$$

where

$$\left[\hat{Q}\right] = [Q] [\Pi_L] \ , \qquad \left[\hat{P}\right] = [\Pi_R] [P], \qquad (2)$$

$[\Pi_R]$ and $[\Pi_L]$ are permutations, $[Q]$ has orthonormal columns, $[P]$ is unitary, $[L]$ is lower triangular and the superscript *H* denotes the conjugate transpose.

Computationally, the *pivoted QLP decomposition* is a two-step application of the *pivoted QR factorization*, first to the FRF matrix $[H]$

$$[H] [\Pi_R] = [Q] [R] \ , \qquad (3)$$

then to the conjugate transpose of the upper triangular matrix $[R] = [Q]^H [H] [\Pi_R]$

$$[R]^H [\Pi_L] = [P] [L]^H. \qquad (4)$$

Substituting $[R] = [\Pi_L] [L] [P]^H$ into $[H] = [Q] [R] [\Pi_R]^H$, one obtains (1).

The pivots $[\Pi_R]$ and $[\Pi_L]$ are permutations to order the diagonal elements of $[R]$ and $[L]^H$, respectively, in the descending order of their absolute value.

Note that $[H]$ is a complex matrix. Algorithms in general use for real matrices can yield negative diagonal elements in $[R]$. They can be made positive and change the sign of the corresponding Q vectors. Next the diagonal elements of $[L]$ can be

negative, requiring a modification of the respective algorithm to track positive values.

The absolute values of the diagonal entries ℓ_{jj} of $[L]$ are called *L-values* [1]. The *L-Values Mode Indicator Function* (LMIF) is the plot of the *L*-values of the FRF matrices $[H(\omega)]_{N_o \times N_i}$ on a log-magnitude scale as a function of frequency. They track the singular values with remarkable fidelity.

The number of LMIF curves is equal to N_i $(N_i \leq N_o)$. The frequencies of the peaks detected in the LMIF plot are estimates of the damped natural frequencies with an accuracy which depends on the frequency resolution.

The orthonormal columns of $[Q]$, referred to as *Q-vectors* (or *Q-Response Functions*), are particular linear combinations of the columns of the FRF matrix

$$\{q\}_k = \sum_{j=1}^{k} s_{jk} \{H\}_j, \tag{5}$$

where s_{jk} are complex valued elements of the upper triangular matrix $[S] = [R]^{-1}$. They are used to generate an enhanced FRF with appropriate scaling.

Let $\{\hat{q}\}_r$ and $\{\hat{p}\}_r$ be the columns of matrices $\left[\hat{Q}\right]$ and $\left[\hat{P}\right]$ evaluated at the *r*-th peak in the LMIF plot. They are used as spatial filters to produce a *Q-enhanced FRF* (QeFRF) for each mode of vibration

$$\{QeFRF(\omega)\}_r = SF_r \{\hat{q}\}_r^H [H(\omega)] \{\hat{p}\}_r \tag{6}$$

where the scale factor

$$SF_r = \begin{Bmatrix} \hat{p}_r(2) \\ \hat{p}_r(3) \end{Bmatrix}^+ \begin{Bmatrix} \hat{q}_r(2) \\ \hat{q}_r(3) \end{Bmatrix} \tag{7}$$

corrects the magnitude and phase of the QeFRF for the *r*-th mode. In (7) the superscript $^+$ denotes the pseudoinverse, while 2 and 3 are the indices of the excitation points.

The effect of this operation is to diminish the contribution of the off-resonant modes in the QeFRF [5].

6. The L-Values Mode Indicator Function

The LMIF plot calculated for excitation in 2 and 50, and response in all 12 lower edge stations is presented in Fig.9. The plot reveals the presence of double modes at 45.75 Hz, 103.3 Hz and 177.8 Hz.

For comparison, the LMIF plot calculated using all 36 measured FRFs, i.e. excitation in three points is shown in Fig.10. It comes out that only two input points are enough to reveal the existence of double modes.

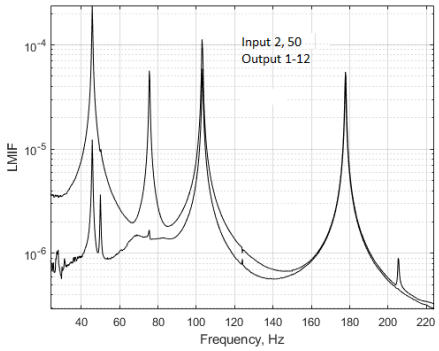

Fig.9. LMIF plot, 2 inputs, 12 output stations

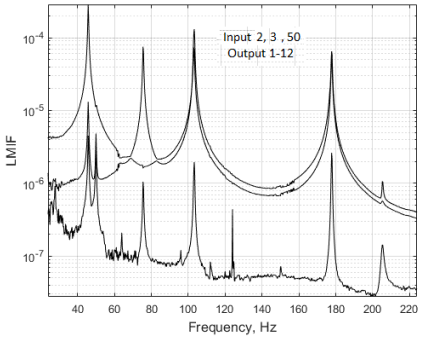

Fig.10. LMIF plot, 3 inputs, 12 output stations

The LMIF plot calculated using only two excitation and two response points, 2 and 3, is presented in Fig.11. Its ability in locating the double modes is remarkable.

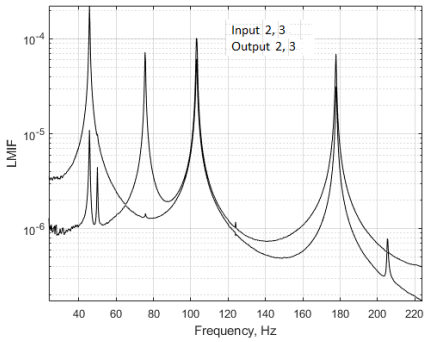

Fig.11. LMIF plot, 2 inputs, 2 output stations

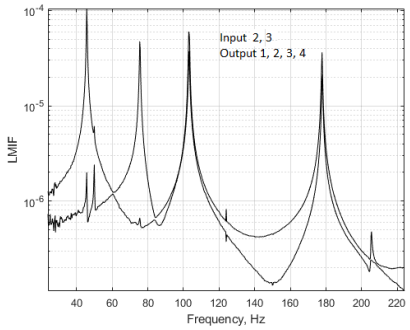

Fig.12. LMIF plot, 2 inputs, 4 output stations

Figure 12 shows the LMIF plot calculated using two excitation and four response points. More output points bring little new information.

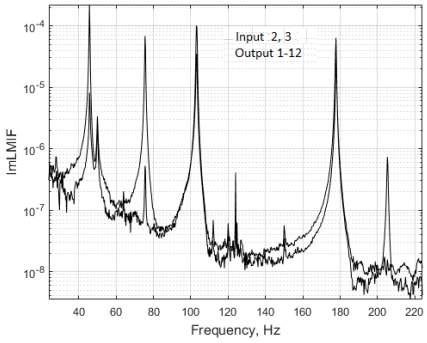

Fig.13. ImLMIF plot, 2 inputs, 12 output stations

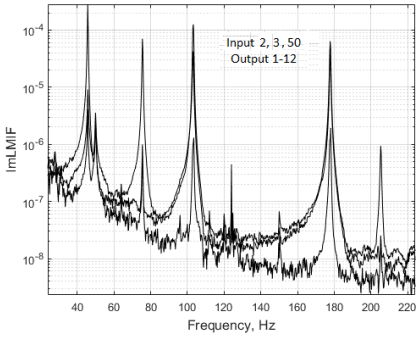

Fig.14. ImLMIF plot, 3 inputs, 12 output stations

Figures 13 and 14 show the ImLMIF plots obtained using in the pivoted QLP decomposition the imaginary part of the FRF matrices. The contribution of the mode at 205.5 Hz is amplified.

7. Analysis of QeFRFs

The QeFRF for mode 1 is presented in Fig.15. It has a dominant peak at 45.75 Hz. The analysis of the Nyquist plot around this frequency is used to estimate the modal frequency and modal damping.
Figure 16 shows the QeFRF for mode 3. It has a dominant peak at 75.5 Hz. The modal frequency and modal damping were estimated by single degree of freedom analysis of the Nyquist plot around this frequency.

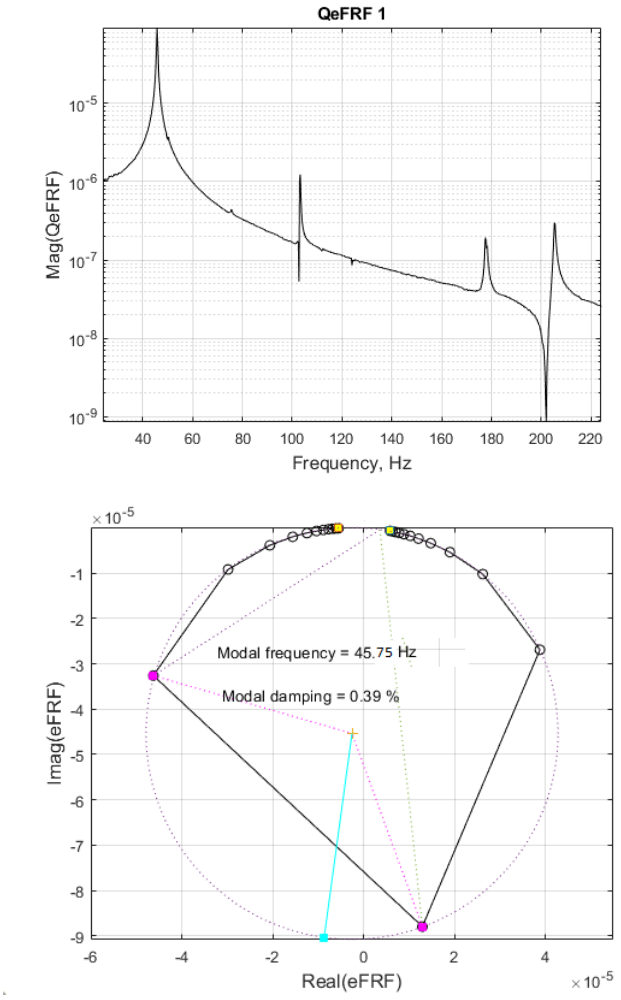

Fig.15. Diagrams of QeFRF1

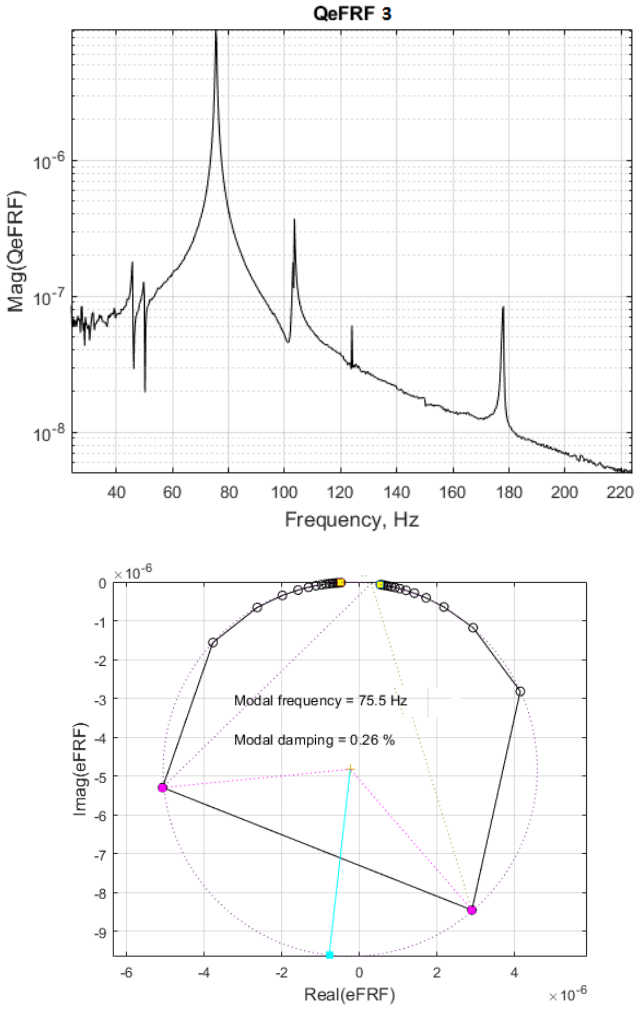

Fig.16. Diagrams of QeFRF3

Despite the low frequency resolution (frequency spacing of only 0.25 Hz), the analysis by circle fitting of the Nyquist plots of the QeFRFs yields good estimates of the modal parameters. This is especially useful for the double modes, for which two different Nyquist plots are analyzed to obtain the corresponding modal parameters, which is not possible analyzing the measured FRFs.

Figures 17 and 18 illustrate the QeFRFs for the two modes at 103.3 Hz. The analysis of the Nyquist plots around this frequency estimates the same values for the modal frequency and modal damping, as expected, despite the obvious low frequency resolution of test data. More data points seem to be necessary around the resonance for a more accurate estimation of modal parameters.

Good results have been obtained using the method of Rational Fraction Polynomials [6].

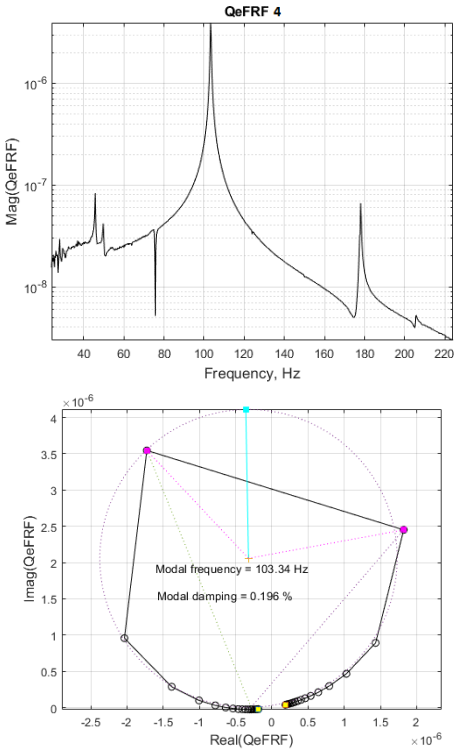

Fig.17. Diagrams of QeFRF4

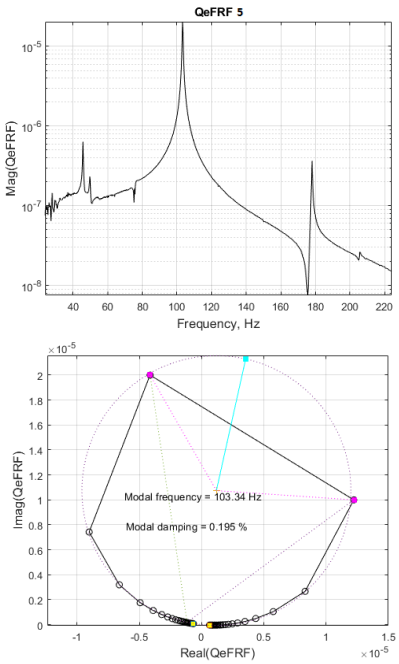

Fig.18. Diagrams of QeFRF5

8. Concluding remarks

The aim of this paper is to document the performance of a new mode indicator function, based on the QLP decomposition with column pivoting of measured complex FRF matrices and the subsequent analysis of enhanced FRFs, in the modal testing of a turbofan case.

The plot of *L*-values versus frequency, referred to as the *LMIF*, has been found to reveal the presence of double modes and give good estimates of the damped natural frequencies, even for a small number of excitation/response stations. Its performance was assessed using measured FRF data for a freely supported axially-symmetric structure.

The LMIF resembles the CMIF as the *L*-values tend to track the singular values of FRF matrices. Similarly, enhanced FRFs have been used to determine the modal parameters.

References

[1] Shih C.Y., Tsuei Y.G., Allemang R.J., Brown D.L., *Complex Mode Indicator Function and Its Application to Spatial Domain Parameter Estimation*, Mechanical Systems and Signal Processing, **2**, 4, 1988, p. 367-377.

[2] Hunt D.L., Vold H., Peterson E.L., Williams R., *Optimal Selection of Excitation Methods for Enhanced Modal Testing,* AIAA Paper 84-1068, 1984.

[3] Stewart G.W., *Matrix Algorithms*, vol.1*: Basic Decompositions*, SIAM, Philadelphia, 1998.

[4] Radeş M., Ewins D.J., *MIFs and MACs in Modal Analysis*, Proceedings of IMAC-XX Conference on Structural Dynamics, Los Angeles, California, Feb 2002, p. 771-778.

[5] Philips A.W., Allemang R.J., Fladung W.A., *The Complex Mode Indicator Function (CMIF) as a Parameter Estimation Method*, Proceedings of the 16th International Modal Analysis Conference, Santa Barbara, California, Feb 1998, p. 705-710.

[6] Maia N.M.M., Ewins D.J., *Modal Analysis of Double Modes: A First Approach to "Intelligent" Curve-Fitting*, Proceedings of IMAC-5 Conference, Imperial College, London, 1987, p. 1302-1308.